HYBRID TEXTURE FEATURES BASED DETECTION AND CLASSIFICATION OF SKIN CANCER USING SIAMESE HETEROGENEOUS BOOSTED SOOTY CONVOLUTIONAL NEURAL NETWORK

Dr. J. Venkatesh¹, Dr. K.Vimalanathan², R. Benschwartz³, Ramapraba P S⁴, R. Selvakumari⁵

¹Professor, Department of Computer Science and Engineering, Chennai Institute of Technology, Kundrathur, Chennai (0000-0002-4259-130X).

Email: venkateshj@citchennai.net, saivimal@annauniv.edu, rbenschwartz87@gmail.com, ramaprabatamilselvan@gmail.com, drselvakumarir@veltech.edu.in,

The unchecked proliferation of aberrant skin cells, typically brought on by UV radiation, is known as skin cancer (SC). It comprises abnormalities including melanoma, basal cell carcinoma, and squamous cell carcinoma that can be cured with early detection and therapy. Identifying SC is crucial, and many techniques are implemented for this purpose. But the existing methods have lot disadvantages such as Poor interpretability and high error rate . To overcome the aforementioned problem, Siamese Heterogeneous Convolutional Neural Network with Boosted Sooty Tern Optimization (SHCNN-BSTO) is proposed for accurately identifying Skin cancer. In this input data is taken from two dataset such as ISIC 2020, ISIC 2019 datasets. Then these data are pre-processed using Sliding Window Variational Outlier-Robust Kalman Filter (SWVRKF) method. Following that, skin cancer region is segmented using the EfficientNet based segmentation method. Then feature extraction are done using Integrating Short-Time Fourier Transform and Continuous Wavelet Transform (STFT-CWT) and optimized with Boosted Sooty Tern Optimization (STO) (SHCNN-BSTO) for detecting the type of skin cancer and to find normal and abnormal region. The introduced system is executed in python. The efficiency of the proposed (SHCNN-BSTO) is analyzed using 2 datasets and attains 99.94% accuracy, 99.56% recall and attains better results compared with the existing methods. This indicates the approach's superior efficiency and potential for further development in the field.

Key words: Skin cancer detection, Sliding Window Variational Outlier-Robust Kalman Filter, Siamese Heterogeneous Convolutional Neural Network, Boosted sooty tern optimization

²Assistant Professor, Department of Industrial Engineering, College of Engineering Guindy, Anna University, Chennai 600 025 (0000-0002-9224-2044).

³Associate Professor, Department of Electronics and Communication Engineering ,Mar Ephraem College of Engineering and Technology, Elavuvilai, Marthandam (0000-0002-2710-2504).

⁴Professor, Department of EEE, Panimalar Engineering college, Chennai (0000-0003-1160-8604).

⁵Assistant Professor, Department of Mathematics, Vel Tech Rangarajan Dr. Sagunthala R & D institute of science and technology, Avadi, Chennai.

Introduction:

A number of factors contribute to the spread of skin cancer, such as population longevity, sun exposure, and early detection of the condition. Dermoscopy, a non-invasive method of skin imaging, used to be one of the best ways to identify skin cancer. Depending on the condition of the skin, a dermoscopic image of a skin lesion may look substantially different from another dermoscopic image. The three layers of skin are the dermis, hypodermis, and epidermis. With melanin absorbing UV rays, it is intended to shield us from dangerous substances and wounds. Anomalies related to aberrant cell proliferation can cause skin cancer and spread to other regions of the body. Melanoma, the most lethal form of the illness, accounts for 75% of skin cancer deaths, despite only 4% of cases.. Skin cancer is mostly caused by ultraviolet radiation from sun exposure. The likelihood of survival rises with early discovery and treatment. Cancers other than melanoma, including SCC, BCC, and SGC, are less likely to spread and are more manageable to treat. Early detection is key to treatment, and computer-based technologies can make it easier, less expensive, and faster to recognize skin cancer symptoms[1-3]. Tumours can be malignant or noncancerous, and they are defined by abnormal cell proliferation. The most common kind of cancer in the world, skin cancer is brought on by abnormal skin cell proliferation. Annually, more than 3.5 million cases are diagnosed—more than lung, bone, and colon cancer combined. Effective prevention requires early detection because there are few therapeutic choices[4-6]. Skin cancer is a frequent malignancy that can affect any area of the skin, especially those that are exposed to the sun. There are a lot of risks involved. Three forms of cancer can be distinguished: melanoma, squamous cell carcinoma, and basal cell carcinoma. Although many people forgo early detection because of a lack of clinics, specialists, resources, or costly treatments, it is vital. Early detection, careful observation, and preventative measures might lessen consequences and their physical repercussions. Professionals or diagnostic instruments such as Dermoscopy can be used to inspect skin lesions. But depending just on the advice of experts can be unreliable. The appearance of the lesion can be affected by image quality, intricacy, and the presence of a skilled expert, among other restrictions with dermoscopy images. Thus, it is advantageous to have a melanoma detection method that is automatic and relies on dermoscopy images[7-9]. The disorder known as skin melanoma is brought on by the abnormal skin cells proliferating quickly, giving the skin a variety of hues and textures. It can be classified as either non-melanoma cancer or malignant melanoma cancer. The most frequent cause of mortality from skin cancer is malignant melanoma. The condition arises from an imbalance of melanocytes in skin cells. Diagnosis is complicated by a lack of agreement, fuzzy borders, and blockages such veins, hairs, and moles.. The difficulties dermatologists encounter when manually visualizing dermoscopic pictures can result in subjectivity and human error. Clinical exams are costly and need for highly qualified medical professionals. To improve the accuracy of cancer detection for medical personnel, researchers are creating computer-aided diagnosis methods[10-12].

Novelty and Contribution

The Novelty and contribution of this paper is given below:

- In this manuscript, a Siamese Heterogeneous Convolutional Neural Networks with Boosted sooty tern optimization (SHCNN-BSTO) based Deep Feature Vectors Concatenation for SHCNN-BSTO is proposed
- The SWVRKF [20] goal is to achieve high filtering accuracy by adaptively adjusting noise covariances to match the properties of input pictures. Its goal is to be less susceptible to data outliers, which can otherwise severely impair the effectiveness of a typical Kalman filter

- Efficient Net based segmentation[21] method was introduced to accurately locate and highlight cancerous areas in skin photographs and also improve skin cancer segmentation. By increasing segmentation map accuracy, this method seeks to enable more accurate skin cancer lesion identification and classification from medical imaging.
- Feature extraction are done using Integrating Short-Time Fourier Transform and Continuous Wavelet Transform (STFT-CWT)[22] for the purpose of extracting the features of skin cancer.
- The objective of employing Siamese Heterogeneous Convolutional Neural Networks with Boosted sooty tern optimization (SHCNN-BSTO)[23] for skin cancer the goal of classification is to increase the precision and effectiveness of medical imaging feature extraction and categorization. This method seeks to improve skin cancer lesion identification and categorization, enabling patients' early diagnosis and treatment planning. Its parameters are optimized through the use of a unique BSTO. [24].

Literature Survey:

In 2023 Qureshi et.al[13] has introduced an convolutional neural networks (CNNs) for detecting skin cancer. The CNN are the foundation of machine learning techniques, which emphasize the importance of early skin cancer diagnosis. Nevertheless, because representative photos are hard to come by, these models sometimes suffer from a lack of data. Multiple CNN models and metadata are combined in a unique ensemble-based CNN architecture, which enhances the models' capacity to handle sparse and unbalanced input. 33,126 dermoscopic photos from 2056 patients were used to test the procedure, and it was compared against seven benchmark approaches.

In 2023 Akram et.al[14] has introduced Skin cancer is identified using a Convolutional Neural Network based on Mask Region (MRCNN). In the context of the Internet of Medical Things (IoMT), this work improves skin lesion analysis using hybrid deep learning techniques. A Mask Region-based Convolutional Neural Network (MRCNN) is used to identify lesions. At 95.49% segmentation accuracy and high accuracy and reliability in skin lesion classification, the model beats existing approaches and shows promise for accurate diagnosis.

In 2023 Venugopal et.al[15] has introduced a deep neural network (DNN) model that uses dermoscopic images to identify skin cancer. This model uses transfer learning, fine-tuning, and data augmentation techniques. The model was trained on 58,032 refined images and outperformed state-of-the-art multiclass classification models. The modified EfficientNetV2-M network enhances the model's performance, ensuring quality services and preventing human errors.

In 2023 Tahir et.al[16] has introduced a diagnosis of skin cancer with the Skin Cancer Classification Network (DSCC_Net), a deep learning-based system. The DSCC_Net outperforms baseline models and offers dermatologists and other medical professional's important support in the diagnosis of skin cancer. DSCC_Net has the following metrics: 99.43% AUC, 94.17% accuracy, 93.76% recall, 94.28% precision, and 93.93% F1-score.

Problem Statement:

Skin cancer must be detected early, but current testing techniques are Poor interpretability, and prone to mistakes. In order to solve this, the ISIC 2020 and ISIC 2019 datasets are used to create the SHCNN-BSTO model, which uses Siamese Heterogeneous Convolutional Neural Networks with Boosted Sooty Tern Optimization for accurate skin cancer identification.

3 Proposed Methodology

Figure 1 illustrates the SHCNN-BSTO operation. The three steps of the suggested method are:(1)pre-processing(2)Segmentation(3) Feature extraction (4) Classification(5)Optimization

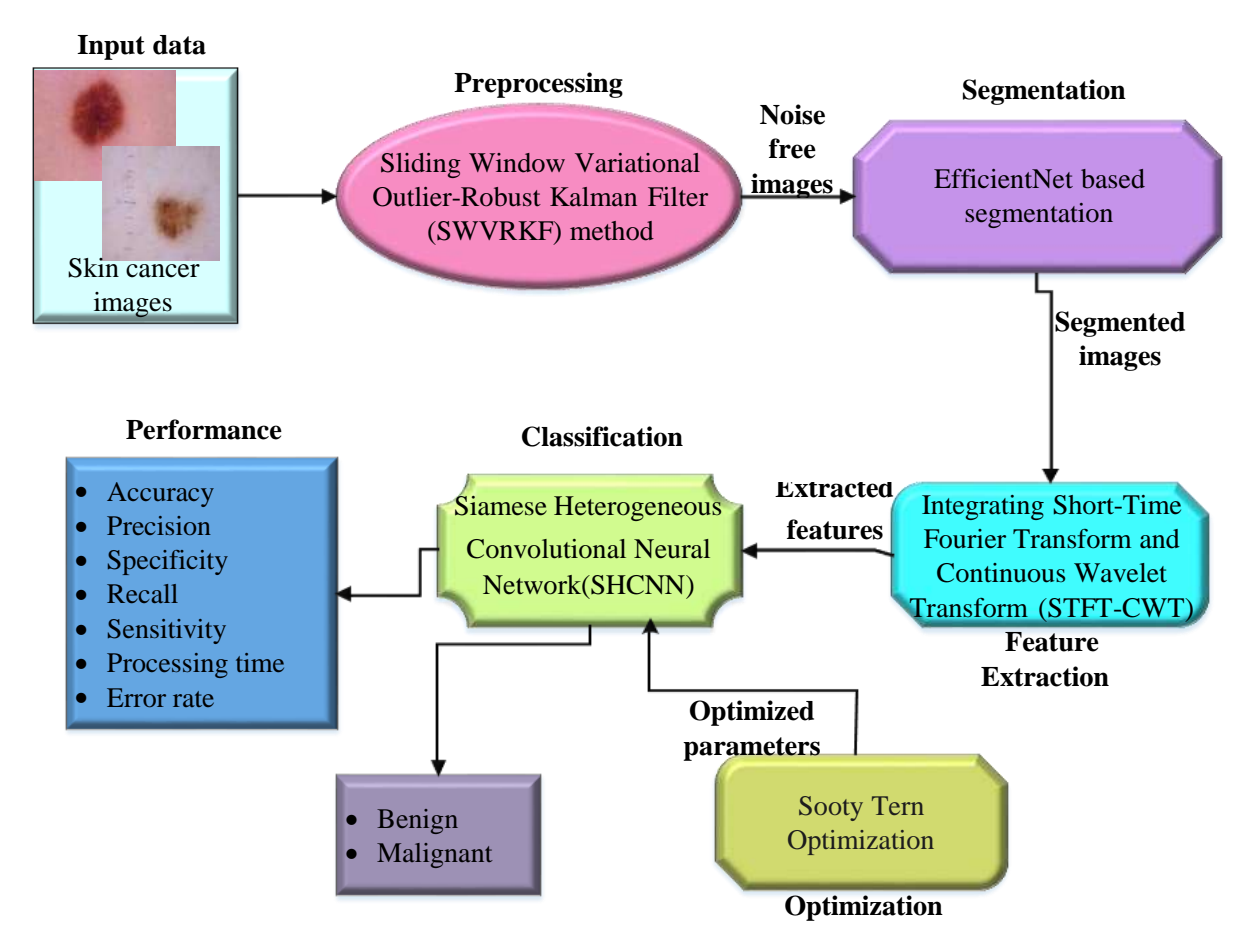


Figure 1: Workflow diagram of proposed SHCNN-BSTO method

3.1 Image Acquisition

In this, to detect skin cancer two types of datasets are taken, they are ISIC 2020 and ISIC 2019 dataset. These images are collected from the scan images, so that, these images are full of noises, to remove these noises pre-processing techniques are used, they are given in next section.

3.2 Preprocessing Using Sliding Window Variational Outlier-Robust Kalman Filter(SWVRKF)

In this, SWVRKF used to pre-process the input skin cancer images for efficient classification[21]. The SWVRKF's goal is to achieve high filtering accuracy by adaptively adjusting noise covariances to match the properties of input pictures. When non-Gaussian noise and outliers are present, the Sliding Window Variational Outlier-Robust Kalman Filter (SWVRKF) seeks to enhance the performance of the conventional Kalman Filter.. The filter's goal is to be less susceptible to data outliers, which can otherwise severely impair the effectiveness of a typical Kalman filter. This work uses Gaussian noise covariance matrix estimation and the sliding window adaptive approach to estimate the scale matrices of the Student's t distributions. The purpose of this suggested SWVRKF is to be different from the current SWVRKF, which aims to address the state estimation problem with unknown or slowly time-varying covariance matrices under Gaussian noises[25-27]. Its objective is to deal with heavy-tailed, non-Gaussian noises tainted by outliers. As such, the sliding window noises in the SWVRKF model have the same covariance matrices and are Gaussian. To combat individual outliers, the noise covariance matrices of the sliding window can be selectively altered by adding the updates of ARVs in comparison to the SWVRKF, as indicated by the algorithm implementations. The computational complexity of the SWVRKF is given in equation(1)

$$S = M \frac{\left[R\left[n^3 + 2p(n^3) + 3n^2m + 4nm^2 + 12m^3 + 2p(m^3) + 3n^2 + 4nm + 7m^2 + 6\right]}{\left[+p(n^3) + p(m^3) + n^2 + m^2\right] + p(n^3) + p(m^3) + 2n^2 + 2m^2 + 2}$$
(1)

where M and R represent the number of iterations and window length, S_{SWRKF} represents the computational process variable, m,n denotes the one dimension input, p represents the asymptotic upper bonds[28,29]. The traditional SWVRKF, a well-known state estimation technique, consists of the time update and measurement update is given in equation (2),

$$\hat{\mathbf{J}}_{L|L-1} = M_L \hat{\mathbf{J}}_{L-1|L-1}$$
 (2)

where, $\hat{Y_{L|L-1}}$ represents the posterior and prior state estimates, M_L denotes the state transition matrix, $\hat{Y_{L-1|L-1}}$ denote the posteriori estimate of the state.

$$N_{L|L} = (R_m - S_L L_L) N_{L|L-1}$$
 (3)

where, $N_{L|L}$ represents the updated error covariance matrix, R_m represents identify matrix,

 $N_{L|L-1}$ represents the predicted error covariance matrix, S_L Kalman gain matrix, L_L represents the observation matrix respectively. Target tracking investigations and simulations show that, at a higher computing burden, the suggested filter outperforms the reliable approaches now in use in terms of tracking accuracy and consistency. By following these procedures, the SWVRKF algorithm can efficiently remove noise from skin cancer images, enhancing both the image quality and the precision of later skin cancer detection techniques. Then to detect the cancer images the particular region is segmented using the Efficient Net based segmentation (E-Net) method, that are discussed in below sections:

Segmentation using EfficientNet:

After pre-processing Segmentation is carried out. Skin cancer segmentation is an essential task in medical image analysis, where the goal is to accurately locate and highlight cancerous areas in skin photographs [22]. Convolutional neural network (CNN) models in the EfficientNet family have gained recognition for their exceptional capabilities and effectiveness in image classification applications. Every model in the EfficientNet series, from EfficientNetB0 to EfficientNetB7, illustrates a different scale of the model architecture with increasing depth, width, and resolution . EfficientNetB0, the baseline model, fairly balances accuracy and processing economy. In applications when resources are limited, it performs admirably.

EfficientNetB0:

A convolutional neural network architecture called EfficientNetB0 is intended for image classification. It is a member of the EfficientNet model family, It attempts to increase accuracy and efficiency by methodically increasing the network's width, depth, and resolution using a compound scaling strategy, given in equation (4)

$$FLOPs = 0.3 \times (M^2) \times N \times (FA + 1) \text{ where, parameters}$$

$$= 0.08 \times (M^2) \times M \times (FA + 1) \dots (4)$$

FLOPs represents the Metrics quantify the amount of floating-point operations needed by an algorithm or its computational complexity, *M* represents the height of the image in an Convolutional neural network, N denotes the number of output channels and *FA* represents the resolution scaling factor

EfficientNetB1:

EfficientNetB1 beats B0 by broadening the model, providing superior performance at a slightly greater computational cost. When compared to B0, it offers a slight gain in accuracy, given in equation (5)

$$FLOPs = 0.4 \times (M^2) \times N \times (FA+1) where, parameters$$

$$= 0.14 \times (M^2) \times M \times (FA+1)..$$
(5)

EfficientNetB2

More width and depth are added to the model by EfficientNetB2, which offers better performance at a little greater computational cost than B1, which is given in equation (6)

$$FLOPs = 0.5 \times (M^2) \times N \times (FA + 1) \text{ where, parameters}$$

$$= 0.17 \times (M^2) \times M \times (FA + 1)$$
(6)

EfficientNetB3

The model's breadth and depth are increased by EfficientNetB3, which raises accuracy but increases computing cost. It outperforms B2 while keeping accuracy and efficiency at a tolerable trade-off, given in equation(7)

$$FLOPs = 0.6 \times (M^{2}) \times N \times (FA+1) \text{ where, parameters}$$

$$= 0.25 \times (M^{2}) \times M \times (FA+1)$$
(7)

EfficientNetB4

The Model B3 is smaller than EfficientNetB4, which has a greater depth and width. Though more processing power is needed, it delivers greater precision given in equation(8)

$$FLOPs = 0.6 \times (M^{2}) \times N \times (FA + 1) where, parameters$$
$$= 0.25 \times (M^{2}) \times M \times (FA + 1)$$
 (8)

• EfficientNetV2M

The upgraded EfficientNet models, known as EfficientNetV2M, take use of developments in architecture design. Compared to their predecessors, they seek to increase both accuracy and efficiency, given in equation(9)

$$FLOPs = 0.35 \times (M^{2}) \times N \times (FA + 1) where, parameters$$

$$= 0.7 \times (M^{2}) \times M \times (FA + 1)$$
(9)

From the segmented images, the image features are detected for identifying benign and malignant region from the given datasets. The feature extraction and classification process are given in next section

Feature extraction using Combining Continuous Wavelet Transform with Short-Time **Fourier Transform (STFT-CWTF)**

After segmentation feature extraction is carried out. From the segmented skin cancer images, the STFT-CWTF is utilized to extract the features of the skin cancer.[23]. Through the use of a windowing function, STFT seeks to achieve a balance between temporal and frequency localization. It splits the signal into manageable chunks and applies a Fourier transform to each chunk. CWT analyzes signals by breaking them down into wavelets, as opposed to the Fourier Transform, and produces a time-frequency representation of the signal's frequency content across time.

Short-Time Fourier Transform

Skin cancer is identified from AE data using a basic signal processing technique called STFT. Shorter segments of the AE signals are reduced, and each section is applied with the FT. This gives signals a complete representation in the time-frequency domain, facilitating analysis of their spectral content and temporal fluctuations. The AE signals' frequency components and their temporal fluctuations must be captured using STFT. This makes it easier to find patterns linked to leaks and typical operating circumstances. A spectrogram, a visual depiction of the energy distribution over time and frequencies, can be used to identify specific patterns and spectral features linked to pipeline breaches. In Skin Cancer detection, window functions and

overlapping can improve resolution and lessen spectral leakage artifacts during STFT calculation. This improves precision, dependability, and efficiency, allowing for proactive pipeline safety measures and well-informed decision-making in industrial applications given in equation (15)

• Continuous Wavelet Transform feature extraction

Using AE signals to analyze two time-series data and find pipeline breakdowns, CWT is a reliable technique for signal processing. When utilized in CWT, wavelets are specialized mathematical functions with localized qualities in the frequency and temporal domains. [16]. A comprehensive representation of the signals in the time-frequency domain is obtained by using CWT.

using CWT.
$$CWT (\sigma, h) = \frac{1}{\sqrt{|R|}} \int_{-\infty}^{+\infty} Y(p)(\lambda) \left(\frac{p - \sigma}{h}\right)$$
(11)

Where, $CWT_Y(\sigma,h)$ denotes the continuous wavelet transform of the signal, $\frac{1}{\sqrt{|R|}}$ represents

the scale parameter, Y(p) represents the analyzation of the signal, λ represents the wavelet function. Then efficiently classifying the skin cancer images in to cancer and non-cancer images. For efficient classification, Siamese Heterogeneous Convolutional Neural Network are used.

Classification using Siamese Heterogeneous Convolutional Neural Networks(SHCNN):

In this, SHCNN is used to extract the features and efficiently classify the skin cancer region with Benign and malignant regions with various datasets using different classes. A particular kind of neural network used for matching and comparing graph-based data is called a Siamese Graph Convolutional Neural Network (Siamese GCN)[24]. It uses a Siamese network structure, which is made up of two weight-sharing subnetworks that are exactly alike. By putting both graph input pairs through the same feature extraction technique, this approach facilitates comparison. The Siamese Network (S-Net) and the Graph Convolutional Neural Network (GCNN), which make up SA-Siam, are explained below.

GCNN

The main objective of this section is to combine the ROI attributes (h_y) to create the best node GV representation and neighbour's features h_y High-level pharmacological information has been extracted by stacking five graph convolutional layers. The ideal dosage of medication is calculated using node classification, and the reaction map is determined using graph classification, which is given in equation (12)

$$h_{\theta} * h_{y} = V * h_{\theta} * h_{y} \tag{12}$$

Where, h_{θ} denotes the convolutional layer filter, V represents the normalized eigenvector graph Laplacian matrix (NEGLM), given in equation (13)

$$M_L = F_O - C_M^{\frac{1}{2}} B_{ii} C_V^{\frac{1}{2}} = V * \eta * V^T$$
 (13)

Where, η denotes the diagonal matrix of eigen values, F_O represents the identity matrix of O_{th} Order, B_{ji} represents the input interaction matrix, C_M and C_V are the lower and upper diagonal matrix of B_{ji} , L represents the represent a modified form of another linear operator or a matrix associated to a graph, V^T denotes the transpose of the eigenvector matrix, M_L denotes the a product of the diagonal and additional matrices, along with identity matrix subtraction. During testing, the weighted normal of the warmth maps from the two branches, given by equation (14), is used to analyze the complete warmth map.

 $g(x', y') = \beta g_r(x, y) + (1 - \beta)g_r(x'y')$ (14) Where, β represents the weighting barrier to modify the two branches respective significance, g(x', y') represents the result of the combination of the two functions, $g_r(x'y')$ denotes the value of the second function (x', y'). Then to improve the classification accuracy, the weight (β) for improving accuracy of SHCNN are optimized using BSTO. The optimization process is given in below section:

3.4.1 Optimization using Boosted sooty tern optimization (SHCNN-BSTO):

Dhiman and Kaur created the STOA algorithm, a novel population-based metaheuristic algorithm, by mimicking the sooty tern seabird's natural migratory and attacking patterns. In the past few decades, it has attracted a lot of interest and has been employed in numerous applications. The attacking/exploitation and migrating/exploration behaviours of sooty sea tern seabirds served as inspiration for the STOA algorithm. Eats include fish, reptiles, insects, earthworms, and more. They are migratory and aggressive creatures that reside in groups. Sooty terns migrate in groups to find the richest areas during their exploration of their new habitat. Sooty terns use flight to find their targets before launching an assault. Typically, they maintain space between each pair of birds to prevent collisions. Birds in a group follow the direction of the most fit or successful survivor and adjust their locations accordingly given in equation(15).

Fitness Function=Maximize (β) (15)

Where, β is used for improving accuracy. Sooty Tern Optimization (STO) is an algorithm inspired by nature that solves optimization problems by imitating the dynamic flocking and seeking behaviors of sooty terns. By decreasing the possibility of becoming trapped in local optima, the enhanced version seeks to deliver more dependable and consistent performance across a range of optimization tasks.

4 Result and Discussions

This section describes the introduced scheme's findings and debate. Python is used to carry out the Result and discussion of the method. Here is some of the Implementation parameter is mentioned in table 1:

Table 1: Implementation Parameters

Parameters	Description
Proposed Neural Network	SHCNN-BSTO
OS	Windows 10
Optimization	BSTO
Dataset	ISIC 2020, ISIC 2019 dataset
Software	Python 3.7

4.1 Dataset Description

To classify the SC, an SC dataset is taken; namely ISIC 2020, ISIC 2019 dataset and its descriptions are given below:

4.1.1 ISIC 2020 dataset

The dataset utilized in the suggested method comprises 33,126 dermatoscopic pictures that were taken from 2056 patients[13]. Based on professional opinion and histopathology, all the photos have been classified as either benign or malignant skin lesions. Although there are another 10982 test data photos in the ISIC 2020 dataset without real labels, since we are focusing on the supervised classification job, we will only be using the labelled data. Every image is in the JPG format, with different sizes and shapes. As a result, we're scale the input photos to sizes of 32×32 , 64×64 , 128×128 , and 256×256 pixels. We employ different input dimensions for different baselers.

4.1.2 ISIC 2019 datasets

This dataset comprises 25,331 dermatoscopic images from the ISIC 2019 collection, which are sporadically distributed among eight classes (kinds of skin illnesses) and include both melanocytic and non-melanocytic skin types[17]. There are 25,331 photos in the ISIC 2019 collection that come from the HAM10000 and BCN_20000 databases. The collection includes details about the lesion's age, sex, and location in addition to high-resolution pictures. There are 10015 RGB images with a resolution of 600 × 450 pixels in the BCN_20000 dataset, in addition to RGB images with a size of 1024 × 1024 pixels. Eight classes, or types, of skin lesions are present in the ISIC 2019 dataset. The ISIC 2019 dataset contains eight classes, or types, of skin lesions :Pictures of 12,875 Nevi (VN) images, 253 Vascular (Vasc) images, actinic keratoses (Akiec), basal cell carcinoma (Bcc), dermatofibroma (Df), melanoma (MEL), and benign keratosis lesions (Bkl) are among the images that are available.

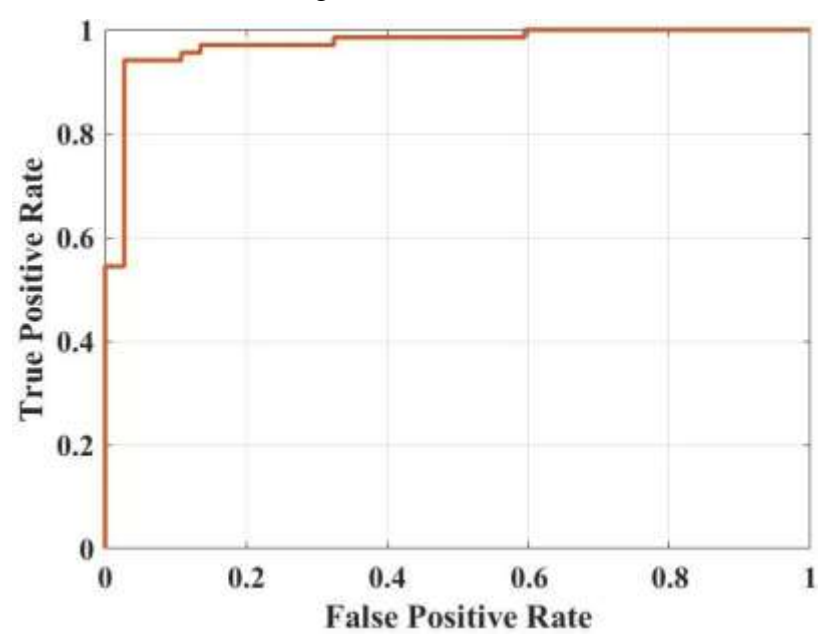


Figure 2: ROC curves Comparisons for proposed approach

Figure 2 shows the of ROC curves Comparisons for proposed approach and the proposed method is compared with existing methods such as CNN[13] MRCNN[14] DNN[15] DSCC_Net[16] AlexNet[17] K-nearest neighbour (KNN)[18] VGG16[19] for ISIC 2020 and ISIC 2019 dataset. A Receiver Operating Characteristic (ROC) curve visualizes a binary classifier system's diagnostic capacity as a function of its discrimination threshold. Figure 3 shows the Confusion matrix for (a) ISIC 2020, (b) ISIC 2019 dataset.



Figure 3: Confusion matrix for (a) ISIC 2020, (b) ISIC 2019 dataset

The confusion matrix's performance analysis is displayed in Figure 1 for (a) ISIC 2020, (b) ISIC 2019 dataset The suggested method performs exceptionally well in identifying real instances and minimizing errors across all datasets, as confirmed by the confusion matrix analysis. This leads to high accuracy, precision, recall, and overall robust performance in SC detection. Table 2 shows the Comparison of performance analysis of proposed approach

Table 2: Comparison of performance analysis of proposed approach

Methods	Dataset	Acc(%)	Pre(%)	Spe(%)	Recall(%)	Sen(%)	PT(%)	Error(%)
CNN[8]	ISIC 2020	90.55	89.95	90.95	87.05	88.4	0.5	0.23
MRCNN[9]	ISIC 2020, ISIC 2019	89.95	90.54	92.45	90.94	88.94	0.6	0.45
DNN[10]	ISIC 2020	78.95	89.04	93.54	88.95	89.04	0.5	0.49
DSCC_Net[11]	ISIC 2020	90.94	88.94	79.94	90.55	89.95	0.4	0.52
AlexNet[12]	ISIC 2019	90.55	89.95	90.95	78.95	89.04	0.5	0.12
KNN [13]	ISIC 2019	90.55	89.95	89.95	90.54	92.45	0.5	0.36
VGG16[14]	ISIC 2019	91.23	87.34	88.56	78.45	93.56	0.3	0.56
SHCNN- BSTO(Proposed)	ISIC 2020, ISIC 2019 datasets	99.94	98.42	99.89	99.56	99.91	0.1	0.10

Here, Acc signifies Accuracy, Pre signifies precision, Spe signifies the Specificity, Sen signifies the sensitivity and PT signifies processing time.

The above Table 2 illustrations the qualified analysis of the proposed method against existing methods CNN[13] MRCNN[14] DNN[15] DSCC_Net[16] AlexNet[17] K-nearest neighbour (KNN)[18] VGG16[19] methods through the ISIC 2020 and ISIC 2019 datasets. The

proposed method attains the highest accuracy (99.94%), precision (98.42%),Spe(99.89%),Recall(99.56%) and Sen(99.91%). It likewise validates the lowest processing time (0.1) ,Error(0.10%) which demonstrating its efficiency and reliability.

5 Conclusion

In this manuscript, SHCNN: a TL-based hybrid texture feature detection and classification system for skin cancer is successfully implemented and discussed. In this input data is taken from two dataset such as ISIC 2020, ISIC 2019 datasets. Then these data are pre-processed using SWVRKF method. Following that, skin cancer region is segmented using the EfficientNet method. Then, using STFT-CWT to extract the skin cancer's features, the abnormal and normal regions are found together with the skin cancer type for classification using SHCNN-BSTO. The introduced system is executed in python. The efficiency of the proposed SHCNN-BSTO is analyzed using 2 datasets and attains 99.91% sensitivity, 0.10% error rate and 0.1s PT and attains better results compared with the existing methods. This indicates the approach's superior efficiency and potential for further development in the field. Future work will enhance model robustness and generalizability by expanding dataset, integrating real-time processing, and creating a user-friendly interface for clinical use.

Reference:

- 1. Ogundokun, Roseline Oluwaseun, et al. "Enhancing skin cancer detection and classification in dermoscopic images through concatenated MobileNetV2 and xception models." Bioengineering 10.8 (2023): 979.
- 2. Shah, Aarushi, et al. "A comprehensive study on skin cancer detection using artificial neural network (ANN) and convolutional neural network (CNN)." Clinical eHealth (2023).
- 3. M. Sughasiny, K.K.Thyagarajan, A. Karthikeyan, K. Sangeetha, K Sivakumar, "A Comparative Analysis of GOA (Grasshopper Optimization Algorithm) Adversarial Deep Belief Neural Network for Renal Cell Carcinoma: Kidney Cancer Detection & Classification," International Journal of Intelligent Systems and Applications In Engineering, ISSN: 2147-6799, 2024, 12(9s), 43–48.
- 4. Gururaj, Harinahalli Lokesh, et al. "DeepSkin: a deep learning approach for skin cancer classification." IEEE Access 11 (2023): 50205-50214.
- 5. Balaji Singaram, Lakshmi. B, Dr.M.Preetha, V.K. Ramya Bharathi, Dr.S.Muthumari lakshmi, Rakesh Kumar Giri "A Smart IoT-Based Fire Detection and Machine Learning Based Control System for Advancing Fire Safety", Nanotechnology Perceptions, ISSN 1660-6795 2024, Vol. 20, 5s, 229-244
- 6. Magdy, Ahmed, et al. "Performance Enhancement of Skin Cancer Classification Using Computer Vision." IEEE Access (2023).
- 7. Aishwarya, N., et al. "Skin cancer diagnosis with YOLO deep neural network." Procedia Computer Science 220 (2023): 651-658.
- 8. Dahou, Abdelghani, et al. "Optimal skin cancer detection model using transfer learning and dynamic-opposite hunger games search." Diagnostics 13.9 (2023): 1579.
- 9. Mukadam, Sufiyan Bashir, and Hemprasad Yashwant Patil. "Skin cancer classification framework using enhanced super resolution generative adversarial network and custom convolutional neural network." Applied Sciences 13.2 (2023): 1210.
- 10. M. Preetha, Archana A B, K. Ragavan, T. Kalaichelvi, M. Venkatesan "A Preliminary Analysis by using FCGA for Developing Low Power Neural Network Controller Autonomous Mobile Robot Navigation", International Journal of Intelligent Systems and Applications in Engineering (IJISAE), ISSN:2147-6799. Vol:12, issue 9s, Page No:39-42, 2024.
- 11. T.Mayavan, S. Sambath, A. Kadirvel, T.S.Frank Gladson, S. Senthilkumar, K Siva Kumar, "Artificial Neural Networks to the Analysis of AISI 304 steel sheets

- through limiting Drawing Ratio test" Journal of Electrical Systems, https://doi.org/10.52783/jes.3463 ISSN 1112-5209 2024, Vol. 20, 4s, 2282-2291.
- 12. Qureshi, Aqsa Saeed, and Teemu Roos. "Transfer learning with ensembles of deep neural networks for skin cancer detection in imbalanced data sets." *Neural Processing Letters* 55.4 (2023): 4461-4479.
- 13. Akram, Arslan, et al. "Segmentation and classification of skin lesions using hybrid deep learning method in the Internet of Medical Things." *Skin Research and Technology* 29.11 (2023): e13524.
- 14. Venugopal, Vipin, et al. "A deep neural network using modified EfficientNet for skin cancer detection in dermoscopic images." *Decision Analytics Journal* 8 (2023): 100278.
- 15. Tahir, Maryam, et al. "DSCC_Net: multi-classification deep learning models for diagnosing of skin cancer using dermoscopic images." *Cancers* 15.7 (2023): 2179.
- 16. Olayah, Fekry, et al. "AI techniques of dermoscopy image analysis for the early detection of skin lesions based on combined CNN features." *Diagnostics* 13.7 (2023): 1314.
- 17. Faizi, Muhammad Imran, and Syed M. Adnan. "Improved segmentation model for melanoma lesion detection using normalized cross-correlation-based k-means clustering." *IEEE Access* (2024).
- 18. Saeed, Mudassir, et al. "The power of generative ai to augment for enhanced skin cancer classification: A deep learning approach." *IEEE Access* 11 (2023): 130330-130344.
- 19. Zhu, Fengchi, et al. "A sliding window variational outlier-robust Kalman filter based on student's t-noise modeling." *IEEE Transactions on Aerospace and Electronic Systems* 58.5 (2022): 4835-4849
- 20. Himel, Galib Muhammad Shahriar, Md Masudul Islam, and Mijanur Rahaman. "Utilizing EfficientNet for sheep breed identification in low-resolution images." *Systems and Soft Computing* 6 (2024): 200093
- 21. Siddique, Muhammad Farooq, et al. "A Hybrid Deep Learning Approach: Integrating Short-Time Fourier Transform and Continuous Wavelet Transform for Improved Pipeline Leak Detection." *Sensors* 23.19 (2023): 8079
- 22. Pati, Soumen Kumar, et al. "Drug discovery through Covid-19 genome sequencing with siamese graph convolutional neural network." *Multimedia Tools and Applications* 83.1 (2024): 61-95
- 23. Saleem, Muhammad Asim, et al. "Sooty tern optimization algorithm-based deep learning model for diagnosing NSCLC tumours." *Sensors* 23.4 (2023): 2147.
- 24. S. B, I. A. Karim Shaikh, P. Jagdish Patil, R. Sethumadhavan, M. Preetha and H. Patil, "Predictive Analysis of Employee Turnover in IT Using a Hybrid CRF-BiLSTM and CNN Model," 2023 International Conference on Sustainable Communication Networks and Application (ICSCNA), Theni, India, 2023, pp. 914-919, doi: 10.1109/ICSCNA58489.2023.10370093.
- 25. A. Jaya Mabel Rani, A Sumalatha, S Annie Angeline Preethi, R Indhu, M. Jayaprakash, M. Preetha, "Innovations in Robotic Technology: A Smart Robotic Design for Effortless Wall Painting using Artificial Intelligence," 2024 International Conference on Automation and Computation (AUTOCOM), , doi: 10.1109/AUTOCOM60220.2024.10486126.
- 26. Srinivasan, S, Hema, D. D, Singaram, B, Praveena, D, Mohan, K. B. K, & Preetha, M. (2024), "Decision Support System based on Industry 5.0 in Artificial Intelligence", International Journal of Intelligent Systems and Applications in Engineering (IJISAE), ISSN:2147-6799, Vol.12, Issue 15, page No-172-178.

- 27. A. Nithya, M. Raja, D. Latha, M. Preetha, M. Karthikeyan and G. S. Uthayakumar, "Artificial Intelligence on Mobile Multimedia Networks for Call Admission Control Systems," 2023 4th International Conference on Smart Electronics and Communication (ICOSEC), Trichy, India, 2023, pp. 1678-1683, doi: 10.1109/ICOSEC58147.2023.10275999.
- 28. Dr.M.Preetha, Balaji Singaram, Dr.I. Manju, B.Hemalatha, P. Bhuvaneswari "Machine Learning in Breast Cancer Treatment for Enhanced Outcomes with Regional Inductive Moderate Hyperthermia and Neoadjuvant Chemotherapy" Nanotechnology Perceptions, ISSN 1660-6795 2024, Vol. 20, 5s, 245-259
- 29. Balaji Singaram, M.S.Vinmathi, Dr.H.B.Michael Rajan, Jeyamohan H, T. Manikandan, "Data-Driven Estimation of Lithium-Ion Battery State-of-Health Prediction Approach Using Machine Learning Algorithm for Enhanced Battery Management Systems", Nanotechnology Perceptions, ISSN 1660-6795 2024, Vol. 20, 7s, 93-103